CHALMERS
UNIVERSITY OF TECHNOLOGY

Enhancing industrial vertical falling film evaporation through modification of heat transfer surfaces – an experimental study

Chemical Engineering & Processing: Process Intensification 191 (2023) 109456

Contents lists available at ScienceDirect

Chemical Engineering and Processing - Process Intensification

journal homepage: www.elsevier.com/locate/cep

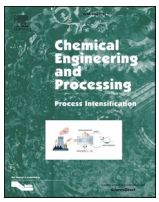

Enhancing industrial vertical falling film evaporation through modification of heat transfer surfaces – an experimental study

Anders Åkesjö [a], Mathias Gourdon [b], Alfred Jongsma [c], Srdjan Sasic [d,*]

[a] Department of Chemistry and Chemical Engineering, Chalmers University of Technology, Gothenburg SE-412 96, Sweden
[b] Valmet AB, P.O. Box 8734, Gothenburg SE-402 75, Sweden
[c] Tetra Pak CPS, Heerenveen, the Netherlands
[d] Department of Mechanics and Maritime Sciences, Chalmers University of Technology, Gothenburg SE-412 96, Sweden

ARTICLE INFO

Keywords:
Falling film
Evaporation
Enhanced heat transfer
Modification of heat transfer surfaces

ABSTRACT

In this study we introduce and experimentally study modifications of heat transfer surfaces as a means to improve the heat transfer in evaporative vertical falling film units. We look at two modified tubular surfaces and compare the obtained results to those acquired using a similar smooth surface. We carry out experiments with two fluids of significantly different viscosities and work with a broad range of industrially relevant operating conditions, with Kapitza (*Ka*) and Reynolds (*Re*) numbers in the range of $Ka = 500–10\,000$ and $Re = 100–2\,000$, respectively. We find that the heat transfer rate in a pilot-scale unit can be improved by 50% to more than 100%, depending on geometrical features (e.g. sharpness) of the modified surface. Our results pave the way for increasing the overall efficiency of industrial evaporation plants by increasing the energy intensity of the evaporator per unit area through carefully tailored modifications of heat transfer surfaces.

1. Introduction

Falling liquid film is a flow situation where a liquid film with a distinct liquid-vapour interface flows down inclined or vertical walls. The thin film gives this technology excellent heat and mass transport characteristics [1]. A falling film unit can operate with small temperature differences and have short residence times and small pressure losses [1]. Therefore, falling film units are a popular choice for a wide range of engineering and technological applications, such as condensers, fluid heaters and chillers, absorbers and evaporators. They are especially good for viscous and heat-sensitive fluids, since they provide relatively good resistance to fouling, due to their possibility to operate with a low thermal driving force.

Falling-film units are frequently used in the food industry for the concentration of heat-sensitive fluids, such as fruit juice and dairy products, to produce fruit juice concentrate and dairy powder. Another area of application is the pulp and paper industry for concentration of black liquor in the chemical recovery process. There, black liquor needs to be concentrated to be burnt in a recovery boiler to recover energy and cooking chemicals when digesting the wood into pulp. These units are typically large, and the heat transfer surfaces are often in the form of long vertical plates or tubes. In addition, thermal separation processes are inherently energy intensive. Thus, improving the energy efficiency of the falling-film technology can substantially improve the overall energy economy of an industrial plant.

Previous studies suggest that enhancing the rate of heat transfer in heat exchangers can be achieved by introducing modifications of heat transfer surfaces [2]. Three courses of action are to be considered: (1) increasing the heat transfer coefficient (HTC) without significantly expanding the heat transfer surface area, (2) enlarging the heat transfer surface without substantial changes of the HTC, and (3) formulating a suitable combination of the previously mentioned scenarios. Generally, the first scenario is preferred due to its cost-effectiveness, as the second one may require additional construction materials for the heat exchanger. However and irrespective of the chosen strategy, it is essential to think about the operational aspects of a heat exchanger when striving to increase the HTC. Factors such as the heat transfer modes (heating, evaporation, boiling, condensation, or cooling), fluid properties, and operating conditions play a vital role in this regard. Also, one should not forget the spatial orientation of the unit, as the fluid flow exhibits variations depending on whether it flows with, against, or perpendicularly to gravity. It is thus recommended that any surface modification is introduced with great caution in order to ensure that the investment in the implemented modified heat transfer surface is indeed meaningful [2].

* Corresponding author.
E-mail address: srdjan@chalmers.se (S. Sasic).

https://doi.org/10.1016/j.cep.2023.109456
Received 21 March 2023; Received in revised form 26 May 2023; Accepted 10 June 2023
Available online 12 June 2023

Nomenclature

Abbreviations

DI	density metre
FI	flow metre
HTC	heat transfer coefficient
Ka	kapitza number
LI	liquid level indicator
Nu	nusselt number
PI	pressure indicator
Pr	prandtl number
Re	reynolds number
TI	temperature metre
VI	viscometer

Symbols

A	area [m^2]
C_p	heat capacity [J/(kg•K)]
d	diameter [m]
g	gravitational acceleration [m^2/s]
h	heat transfer coefficient [W/(m^2·K)]
k	thermal conductivity [W/(m·K)]
L	characteristic length [m]
$\dot{m}$	mass flow rate [kg/s]
P	pressure [Pa]
Q	heat flux [W]
q	heat flux [W/m^2]
T	temperature [K]
U	overall heat transfer coefficient [W/(m^2·K)]
$\dot{V}$	volumetric flow rate [m^3/s]
Γ	wetting rate, mass flow rate per unit width [kg/(m·s)]
ΔH_{Vap}	enthalpy of vaporization [kJ/kg]
ΔP	pressure difference [Pa]
ΔT	temperature difference [K]
δ	thickness [m]
μ	dynamic viscosity [Pa·s]
π	Pi
ρ	density [kg/m^3]
σ	surface tension [N/m]

Subscripts

c	condensation
e	evaporation
i	inner
m	logarithmic mean
o	outer
w	wall

Superscripts

*	saturated

There are no specific design recommendations available for vertical falling film units [3]. Due to a wide range of applications where falling films are used, it is challenging to establish their universal design concept. However, a few studies have explored heat transfer enhancement through modified surfaces in vertical falling films. Gambaryan-Roisman and Stephan [4] investigated the effect of initiating a micro evaporation region on a grooved surface in order to alter the heat transfer mode. Gambaryan-Roisman, Yu, Löffler, and Stephan [5] aimed to improve heat and mass transfer by introducing microscale surface modifications. Pecherkin, Pavlenko, and Volodin [6] examined the effect of introducing small diamond-shaped ridges, especially when low-viscosity fluids are to be used. Although changing the heat transfer mode to a nucleate boiling one can be effective for enhancing the heat transfer, it may not be suitable for all operating situations. One of the main reasons for this is that the temperature driving force is often insufficient to induce nucleate boiling for heat-sensitive fluids, and microstructures can be exposed to impurities and prone to fouling.

Changes in the liquid flow pattern as a result of introducing surface modifications were detected by Li, Yi, Li, Pavlenko and Gao [7] and Slade, Veremieiev, Lee and Gaskell [8]. Yu, Löffler, Gambaryan-Roisman and Stephan [9] concluded that with a grooved surface the wall temperature was lower for fluid heating. Najim, Feddaoui, Nait Alla and Charef [10] used a sinusoidally-shaped heat transfer surface in their computations and the study resulted in a significantly improved rate of evaporation. Raach and Mitrovic [11] made a numerical study of how wires disturb the flow pattern for water desalination on vertical plates. They identified an optimum spacing of Ligament to Height = 18 between the surface modifications. The authors did not discuss in detail the underlying mechanisms, but noted a 100% increase of the evaporation rate. Salvagnini and Taqueda [12] applied a wire mesh to the heat transfer surfaces and studied the effects on the heat transfer when water is employed as a working fluid. They found that the evaporation rate could be triplicated.

Broniarz-Press [13] investigated mass transfer on spirally threaded tubes. The study showed that the rate of mass transfer increased 2–3 times compared to the case with a smooth tube. Shen, C.H. and F. [14] saw the same increase for mass and heat transfer on their vertical screw grooved tubes and claimed that such an increase was caused by recirculation zones within the liquid. Zheng and Worek [15] studied heat transfer in case of inclined falling films on a modified surface, and also claimed that the observed improvement was caused by recirculation zones within the liquid. Ramadane, Goff and Liu [16] looked at the rate of evaporation of a vertical falling film on a surface with large surface fins. The improvement was mainly caused by the increased surface area, with the authors also pointing to an existence of a secondary enhancement mechanism, namely due to the non-uniformity of the flow caused by the fins.

Goff, Soetrisnanto, Schwarzer and Goff [17] and Bandelier [18] proposed a new concept with large moving spiral fins and found an heat transfer increase of 350%. The authors claimed that the increase was caused by the radial mixing caused by the fins. Kohrt [19] studied CO2 absorption into silicon oils on different plate structures in a lab-scale unit. They found that the mass transfer was increased by 30–75% depending on the fluid viscosity. The same study also noted a three-dimensional (3D) nature of the flow, but as the modified surfaces were also made of 3D structures this effect is not surprising. Zhao and Cerro [20] studied the influence of several characteristics for corrugated surfaces for a packing material with the thin film flow in a small experimental facility. Miriam [3] investigated the effect of a vertical grooved surface (longitudinally grooved) and a recorded a heat transfer improvement of around 40%. Schröder, Fast and Sander-Beuermann [21] looked at longitudinal structures for a Na-Cl solution and water respectively, and found an increase in the range of 2–3 times compared to that on a smooth surface. Helbig, Nasarek, Gambaryan-Roisman and Stephan [22] investigated the influence on the hydrodynamics of the implementation of mini grooves aligned with the main flow direction.

The cited works make it evident that introducing surface modifications is a promising way to increase the rate of heat transfer in vertical falling film units. It also seems that modifications introduced perpendicularly to the flow are especially promising as they have been shown to affect the most the flow pattern of the liquid film [3]. We argue here that the full effect on the flow is not yet fully clear of the wide range of operating conditions, operations at large scale and the exact shape of surface modifications. Only after considering the mentioned conditions,

a strategy for designing an industrial falling film unit can be formulated.

In a recent study we have also shown that it is possible to significantly increase the rate of heat transfer in a falling film unit by introducing modifications of heat transfer surfaces [23]. The study comprised both experiments and numerical simulations and showed that the rate of heat transfer could be improved by a factor of 2.5, compared to a corresponding smooth surface. The numerical simulations involved a direct solving of the full Navier-Stokes equations in two dimensions, using the volume of fluid (VOF) numerical framework to resolve the flow structures in the liquid film. The increase in the heat transfer was explained by the appearance of significantly enlarged time-dependent recirculation zones occurring behind the surface modifications [23]. However, that study was limited to heating conditions, and since there are important differences between heating and evaporation in the context of vertical falling film units, we need to prove that the concept works also for evaporative conditions at an industrially relevant scale. The objective of this study is thus to experimentally investigate the potential heat transfer improvement in a falling film evaporator, at an industrially relevant scale, by introducing surface modifications to the heat transfer surface.

Due to different boundary conditions during heating and evaporation, the resulting transport resistance and the subsequent temperature profiles within the liquid film differ significantly [1]. The latter profiles for heating and evaporative conditions for laminar and turbulent films can be described according to Fig. 1 (Schnabel and Schlünder [24]). For a Turbulent film, most of the heat transport resistance resides in the boundary layer close to the wall for both heat transfer modes. For Laminar flow conditions, the temperature profiles within the film are different. For the evaporative case, the temperature profile is a straight line, while for heating it has a more exponential decline indicating a heat transfer resistance throughout the whole film.

The operating conditions for an industrial falling film unit typically result in the Wavy-Laminar or Transition regime, where the heat transfer usually is described as mixture between purely Laminar and Turbulent film flow.

In an evaporator, vapour is produced by the evaporation process. The vapour will cause a gas flow that in turn will give rise to a pressure drop, ΔP. The pressure drop will affect the local saturation temperature (T^*) of the liquid along the surface. Provided that the steam temperature is constant, this will lead to a larger thermal driving force ($\Delta T = T^*_{steam} - T^*$) at the bottom of the evaporator compared to that at the upper part (see Fig. 2); thus, it will directly influence the amount of the transferred heat. The pressure drop will be of importance especially if the flow runs on the inside of a tubular heat exchanger design [26,27].

The vapour flow does not only cause a pressure drop, but it will also affect the falling film hydrodynamics and, consequently, the heat transfer. In a co-current flow, where the vapour exits at the bottom (see Fig. 2), the film can be attenuated and accelerated due to friction at the liquid-gas interface [28]. At what vapour flow the liquid film is significantly impacted is however still debated and depends heavily on the operating conditions [29]. In addition, during evaporation, bubbles on the liquid-gas interface can form which significantly affects both the heat transfer and pressure drop [30,25].

2. Method

The experiments were performed in the Chalmers single-tube pilot evaporator, see Fig. 3. The evaporator has two configuration modes, with the product flow on the outside or inside of the tube, the latter being used in this study. The pilot evaporator is designed to be large enough to give industrially relevant results and, at the same time, small enough to be flexible and controllable. Condensing steam is used as the heat supply and approximately 0.050 m^3 of liquid is needed to run the facility. For the interested reader, further details from other investigations performed with this pilot evaporator can be found in the works of Johansson, Olausson and Vamling [31], Gourdon, Karlsson, Innings, Jongsma and Vamling [32], Gourdon, Innings, Jongsma and Vamling [25] and Karlsson, Gourdon and Vamling [33].

A flowsheet of the pilot evaporator setup used in this work can be seen in Fig. 4. The main component is a 4.125 m long stainless-steel tube with an internal diameter (d_i) of 48.6 mm, an external diameter (d_o) of 51 mm and a total outside heat transfer area (A_o) of 0.66 m^2. The liquid flows on the inside and steam condenses on the outside to supply heat. The volumetric flowrate of the condensate is measured by two level switches with a known volume and used to calculate the rate of heat transfer. The tube is enclosed in a shell that is well isolated from the

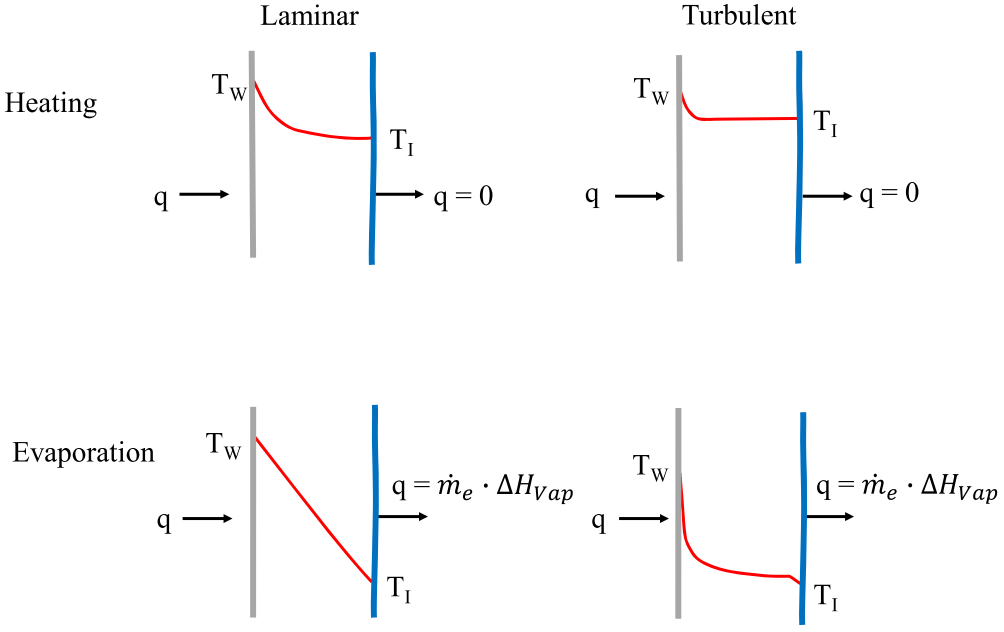

Fig. 1. Temperature profiles within a flat film for laminar and turbulent flows, depicted both for heated and evaporative conditions according to Schnabel and Schlünder [24]. For surface evaporation, which is the typical heat transfer mode for falling film evaporation [25], the interface temperature (T_I) is equal to the saturation temperature (T^*).

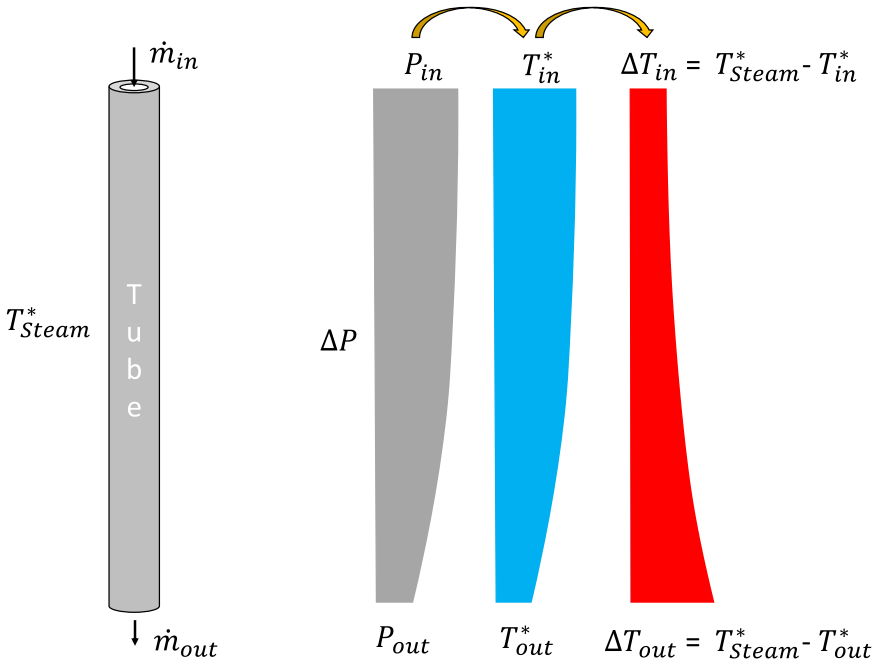

Fig. 2. Schematic representation of the effect of the pressure losses (ΔP) on the saturation temperature (T^*) and the thermal driving force (ΔT) over a heat -transfer tube with the flow on the inside and the condensing steam on the outside of the tube.

Fig. 3. Pilot evaporator used in this work.

surroundings.

The liquid is fed to a buffer tank and then recirculated over the tube by a pump. An overflow distributer on the top guarantees an even distribution of the liquid under all experimental conditions. The liquid and the evaporated vapour exit at the bottom of the tube. The liquid is collected in a cup in order to measure the mixed cup temperature of the liquid (T_{out}). By experience, however, the measured mixed cup temperature is closer to the saturation temperature of the outgoing liquid, T^*_{out}, than to that of an actual mixed cup. The flow of liquid and gas within the tube results in a pressure drop between the tube inlet and outlet, which is measured by a differential pressure metre. This of course influences the thermal driving force. The thermal driving force is controlled by specifying the pressure on the steam side (corresponding to the desired steam saturation temperature, T^*_{steam}) and the liquid outlet temperature. The vapour flows to a condenser where it is condensed and then returned to the buffer tank to maintain constant fluid properties during the experiments. The evaporator is equipped with numerous additional sensors, such as those for measuring pressure and temperature, in order to ensure and monitor stable operating conditions. Note that only the ones used for the analysis presented in this work are shown in Fig. 4.

The evaporator setup comprises a large number of measurement devices, see Fig. 4. An overview of these devices, together with their accuracy can be seen in Table 1.

To investigate the effect of different heat transfer surfaces, the tube can be replaced. The grey bolts seen on the flanges of the evaporator in Fig. 4 can all be untied to remove the heat transfer tube through the bottom of the shell casing. The tubes selected for testing have a flange welded on the bottom part and a cylinder welded on the top to perfectly seal the steam side from the product side. The cylinder acts both as a distributor for the liquid to flow smoothly over the top edge, and as a smooth surface for the O-ring to seal the steam side from the liquid side. This construction allows for thermal expansion of the material without damaging the heat transfer tube. This ensures that different tube designs can be repeatedly tested without the need for rebuilding the evaporator.

Based on our previous work [23], we have in this study investigated under evaporative conditions two modified surfaces, a *Corrugated* and a *Welded* surface, together with a smooth surface, see Fig. 5. We motivate our choice by wanting these surfaces to be similar to the ones investigated in [23] and, at the same time, be possible to manufacture at an industrial scale, with either the currently available manufacturing methods [34] or those that will be available in the future. Due to the employed manufacturing technique, the *Corrugated* surface has an area increase of about 3% on both the steam and the product side compared to a smooth surface. Meanwhile, the *Welded* surface has a zero increase on the steam side and 16% on the liquid side. The *Welded* surface is

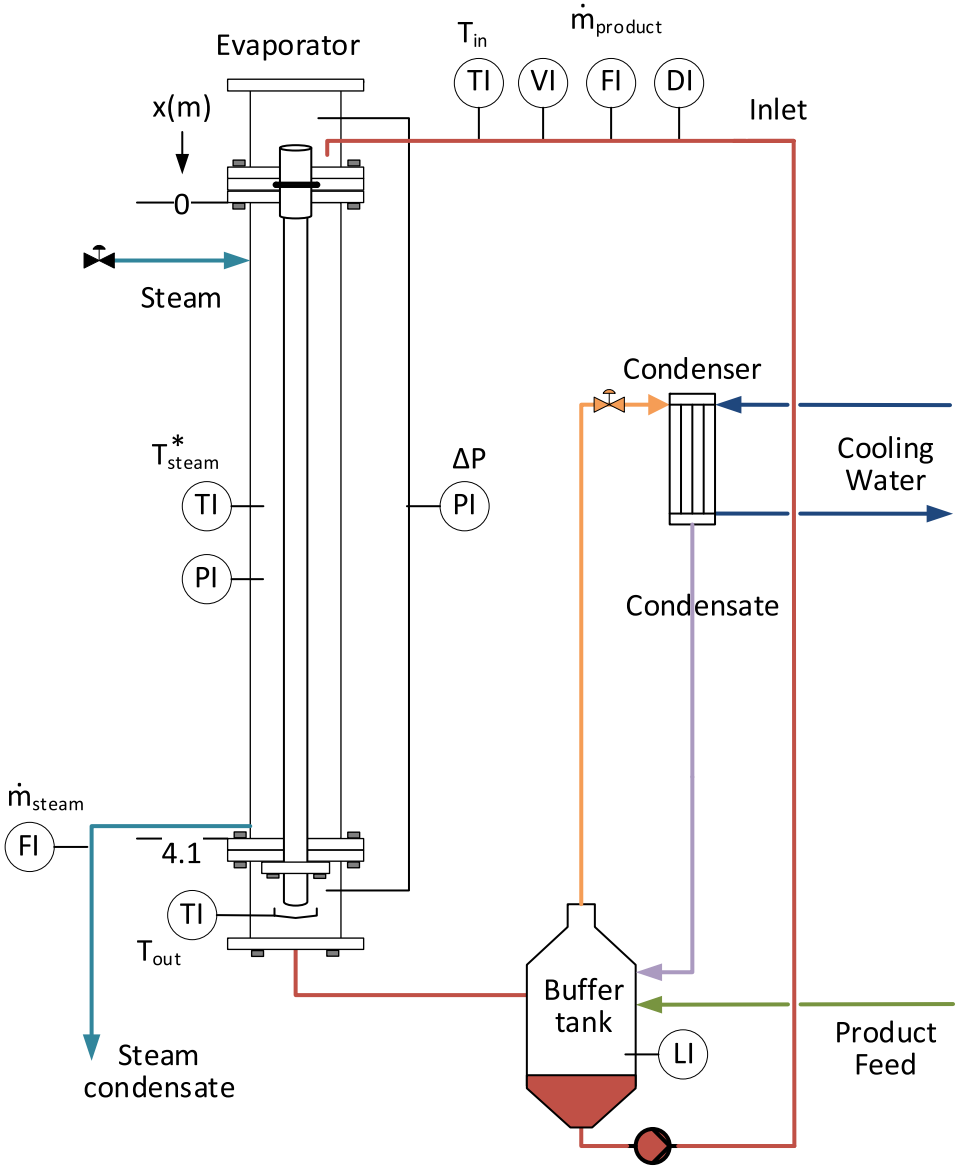

Fig. 4. Simplified flowsheet of the pilot evaporator setup used in this work. LI = Liquid level indicator, PI= Pressure indicator, DI= Density metre, FI=Flow metre, TI=Temperature metre, VI=Viscometer.

Table 1
Information on measurement instruments and their accuracy.

Quantity	Instrument	Accuracy
Temperature	TC, Pentronics type K PT-100 H210, ABB H210, H600	± 0.05 K after calibration
Liquid mass flow rate	PROline promass 80 H, Endress + Hauser	± 0.15% of range
Density	PROline promass 80 H, Endress + Hauser	0.5 kg/m^3
Viscosity	Viscoscope–Sensor VA-300 L, Marimex	± 1.0% of value
Pressure	Yokogawa EJA530, EJA510, EJA110	± 0.2 of range
Volumetric steam condensate	Method: Measure time between two levels with known volume with two VEGASWING 61 vibrating level switches	

sharper compared to the *Corrugated* one and is expected to have a greater impact on the rate of heat transfer based on previous experience [23].

Two types of fluids were investigated in the Pilot evaporator, *Water* and a more viscous industrially relevant fluid (termed here *Industrial fluid*), both at 70 °C (for both inlet and outlet temperatures). All fluid properties and operating conditions are specified in Table 2. The steam temperature was altered in order to change the heat flux (q_e).

2.1. Evaluation procedure

First the volumetric flowrate is converted to the mass flow rate:

$$\dot{m}_{steam} = \dot{V}_{steam}\, \rho_{steam}\ . \tag{1}$$

Afterwards, the heat transfer is evaluated by calculating the heat flux (q_e) from the steam condensate mass flow ($\dot{m}_{steam}$), the enthalpy of vaporization (ΔH_{Vap}), the outside area (A_o) and the subtraction of losses to the surroundings (Q_{losses}), measured prior to the experiments as a function of the steam temperature (approximately 1 kW at 80 °C). Practically, this is done by heating the steam side to the desired temperature and calculating the steam condensate mass flow without having any evaporation or product on the product side:

$$q_e = \frac{\dot{m}_{steam}\Delta H_{Vap} - Q_{losses}(T_{steam})}{A_o}\ . \tag{2}$$

The heat flux is then used to calculate the overall heat transfer coefficient (U):

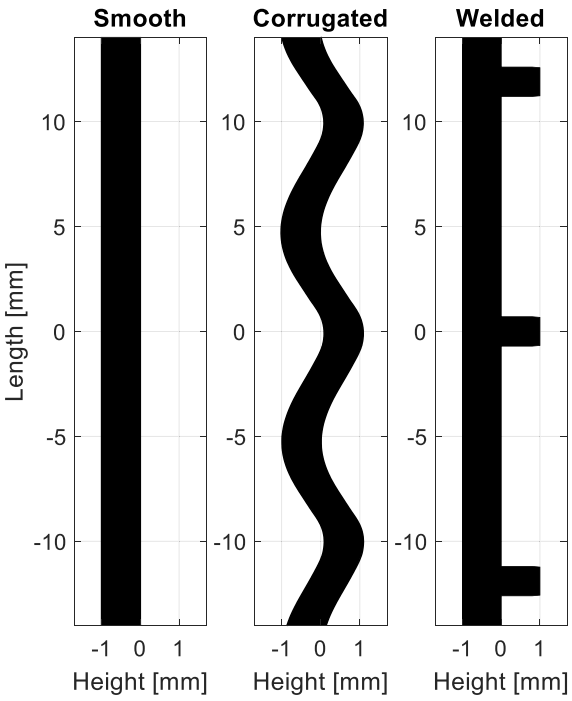

Fig. 5. Cross section view of the smooth surface and the two modified heat transfer surfaces investigated in this study. The origin of the coordinate system in this figure has been placed at the centre of the surface modification and where the original smooth tube surface is or where it would have been if there were no modification.

$$U = \frac{q_e}{\left(T^*_{steam} - T_{out}\right)} \ . \tag{3}$$

This evaluation method directly indicates how high the rate of heat transfer is without the need for any modelling of, for example, the transport resistance on the steam side. The procedure also includes the effect of the pressure drop since the largest temperature difference is used as the driving force, as described in the introduction. We also note that this is how performance of a real industrial unit is evaluated. The latter question is far from straightforward–Cyklis [37] looked into how reliable the estimations for the overall heat transfer coefficients are for falling film evaporators under realistic, industrial-scale operating conditions. The study identified rather divergent results when having compared the measured values with those obtained by some of the currently used expressions.

We argue that the suggested procedure works well as an evaluation tool as long as the ratio of the tube length over the heat transfer area is constant, which has been the case for all the experiments with the pilot evaporator (we remind the reader here that we neglect here the area increase due to the surface modifications). Our definition of the overall heat transfer coefficient differs slightly from what is typically done in the literature for the cases with significant pressure drops [38]. It is desirable for the overall heat transfer coefficient to be independent of the tube length and comparable with other experimental setups of different sizes. However, in order for us to work with such a definition of U, the temperature profile in the evaporator needs to be known. Since we cannot measure the temperature profile, a large experimental data set would be required to properly estimate the profile [27]. Therefore, one can view our definition of the overall heat transfer coefficient for these cases more as a performance indicator. However, in order to compare with other published work, it is possible to use the Nusselt number:

$$Nu = \frac{hL}{k}, \tag{4}$$

together with the following expression for the overall heat transfer coefficient:

$$U = \frac{1}{\left(\frac{1}{h_e A_i} + \frac{\delta_w}{k_w A_m} + \frac{1}{h_c A_o}\right) A_o}, \tag{5}$$

where h_e is the heat transfer coefficient of the evaporating liquid, A_i is the heat transfer area on the inside of the tube, k_w is the conductivity in the tube wall estimated with the procedure suggested by Assael and Gialou [39], since it is representative for the material that the tube is constructed of:

$$k_w = 14.22\left(0.3989 + 0.72\frac{T_{steam}+25}{298.15} - 0.1188\left(\frac{T_{steam}+25}{298.15}\right)^2\right). \tag{6}$$

In expression (5), h_c is the heat transfer coefficient of the condensing steam which was estimated using a correlation for condensation on vertical surfaces by Numrich and Müller [40]:

$$Nu_{c,Laminair} = 0.925\left(\frac{\left(1 - \frac{\rho_{Vapour,c}}{\rho_{liquid,c}}\right)}{Re_c}\right)^{1/3},$$

$$Nu_{c,Turbulent} = \frac{0.020 Re_c^{\frac{7}{24}} Pr_c^{\frac{1}{3}}}{1 + 20.52\ Re_c^{-\frac{3}{8}} Pr_c^{-\frac{1}{6}}},$$

$$Nu_c = \left(\left(Re_c^{0.04}\ Nu_{c,Laminair}\right)^{1.2} + Nu_{c,Turbulent}^{1.2}\right)^{\frac{1}{1.2}}. \tag{7}$$

The logarithmic mean area A_m is calculated in the following way:

$$A_m = \frac{A_o - A_i}{ln(A_o/A_i)} \ . \tag{8}$$

2.2. State of the art related to heat transfer on smooth surfaces

The knowledge about the rate of heat transfer on commercially available smooth surfaces is relatively well documented and best summarized in correlations developed from experimentally measured data. These correlations are of great use to compare our work with, since such comparisons will directly indicate how industrially significant our results are. Johansson, Vamling and Olausson [41] made a thorough compilation and comparison of correlations available in the literature and suggested that the correlations provided by both Schnabel and Schlünder [24] and Numrich [42] should be used.

The correlation proposed by Schnabel and Schlünder [24] expresses

Table 2
Operating conditions for the fluids investigated in the Pilot evaporator setup. All values are measured if not specified otherwise. All experiments were performed at 70 °C (Outlet temperature).

Fluid	μ mPas	ρ kg/m^3	k W/(m•K)	C_p J/(kg•K)	σ N/m	Ka –	Pr –	Re –	Γ kg/(m•s)	P_{out} Pa
Water	0.40	978	0.66[a]	4185[a]	0.0647[a]	10,053	2.5	250–2000	0.18–1.1	31 000
Industrial fluid	2	1167	0.58[b]	3600[b]	0.025[b]	480	13	88–490	0.18–0.9	35 000

[a] Value obtained from NIST [35].
[b] Value obtained from Adams, Frederick, Grace, Hupa, Lisa, Jones and Tran [36].

the Nusselt number (*Nu*) variation in terms of the Reynolds (*Re*) and Prandtl (*Pr*) numbers:

$$Nu_{Evaporation} = \sqrt{(0.90 \cdot Re^{-1/3})^2 + (0.00622 \cdot Re^{0.4} \cdot Pr^{0.65})^2}. \quad (9)$$

The correlation was based on measurements conducted for different fluids with Prandtl numbers in the range of 1.75–7, and its accuracy estimated to be ± 20%. Numrich [42] proposed a slightly modified version for Prandtl numbers of up to 52:

$$Nu_{Evaporation} = \sqrt{(0.90 \cdot Re^{-1/3})^2 + (0.0055 \cdot Re^{0.44} \cdot Pr^{0.4})^2}. \quad (10)$$

Numrich did not explicitly state the accuracy but, based on the data provided in the publication, the accuracy can be expected to be around ± 25%.

Recently, Gourdon, Karlsson, Innings, Jongsma and Vamling [32] have also proposed a modified version of the relation for Prandtl numbers in the range of 3–800:

$$Nu_{Evaporation} = \sqrt{(0.90 \cdot Re^{-1/3})^2 + (0.011 \cdot Re^{0.2} \cdot Pr^{0.65})^2}. \quad (11)$$

The authors compared their correlation to measurement data in the literature and found that the correlation could successfully reproduce the measurements with an accuracy of ± 30–40%.

These correlations can therefore be used to compare with our experimental results. Preferably our measurements on a smooth surface should be within their margin of error and the results from the modified surfaces should exhibit a significant difference for us to be able to claim a substantial heat transfer improvement.

3. Results and discussion

The overall heat transfer coefficients, calculated from Eq. (3) for the two investigated fluids, at $\Delta T_{out} = 10$ K and at various wetting rates for the investigated surfaces, can be seen in Fig. 6. The correlations developed for smooth surfaces by Schnabel and Schlünder [24], Numrich [42] and Gourdon, Karlsson, Innings, Jongsma and Vamling [32] are also included as a reference, but only for the fluids that they are valid for. Their resulting overall heat transfer coefficients are calculated from Eqs. (4) and (5).

It is clear from the measurements that there exists an improvement to the rate of heat transfer by using modified heat transfer surfaces. For the Industrial fluid Fig. 6, left), the improvement is around 30% for the *Corrugated*-, and 40% for the *Welded* surface. For *Water* (Fig. 6, right), the improvement on the *Corrugated* is 25% and up to 60% for the *Welded* surface. There is a certain degree of dependence on the wetting rate for these numbers, but we overall note a significant improvement to the rate of heat transfer. A wetting rate dependence was also found in our previous study that focused on heating instead of evaporation [23]. However, in that case the heat transfer improvement was close to zero at lower wetting rates. The time-dependant recirculation zones that appeared behind the surface modifications which were the cause for the enhancement, did not exist at lower wetting rates. Since the heat transfer clearly is also enhanced at lower wetting rates on the modified surfaces with the evaporation present, we hypothesize the existence of an additional mechanism taking place here as compared to heating.

An increase in the heat transfer rate caused by modification of surfaces will result in a higher heat flux. The higher heat flux implies more liquid evaporated, causing a higher vapour flow and resulting in a larger pressure drop and a lower temperature driving force, and potentially leading to a thinner liquid film [43]. In addition, for the *Industrial fluid*, the fluid properties will change at a higher rate if more vapour is evaporated, since the dry solids content of the outgoing fluid will be higher. Therefore, a more straightforward evaluation of the improvement rate is to compare measurements at the same heat flux, see Fig. 7.

The heat flux in Fig. 7 was controlled by changing the thermal driving force, ΔT_{out}, or more specifically T_{steam}. Since ΔT_{out} is only varied between 2.5 and 10 K, it has only small effects on the fluid properties. All measurements are conducted at the same volumetric flow rate of 300 l/h and here an even larger heat transfer improvement can be seen for the modified surfaces (Fig. 7). For the *Industrial fluid*, the improvement is around 50% for the *Corrugated*, and 100% for the *Welded* surface if compared at approximately the same heat flux. For *Water*, the same numbers are 30% and 90%, respectively. The values for the modified surfaces are high and seem to increase for lower heat fluxes. It should be noted that q_{losses}, which is used to account for the losses in the evaporator, is around 1 kW (or 1.5 kW/m^2 if divided by the heat transfer area), and therefore, the lower the heat flux, the larger are the uncertainties. However, that does not explain the trend seen in the data points and further methods of evaluating the results are needed. The area increase due to the modification of the surface is relatively minor compared to the total heat transfer improvement. For the *Corrugated* surface this increase is approximately 3% on both in- and outside and for

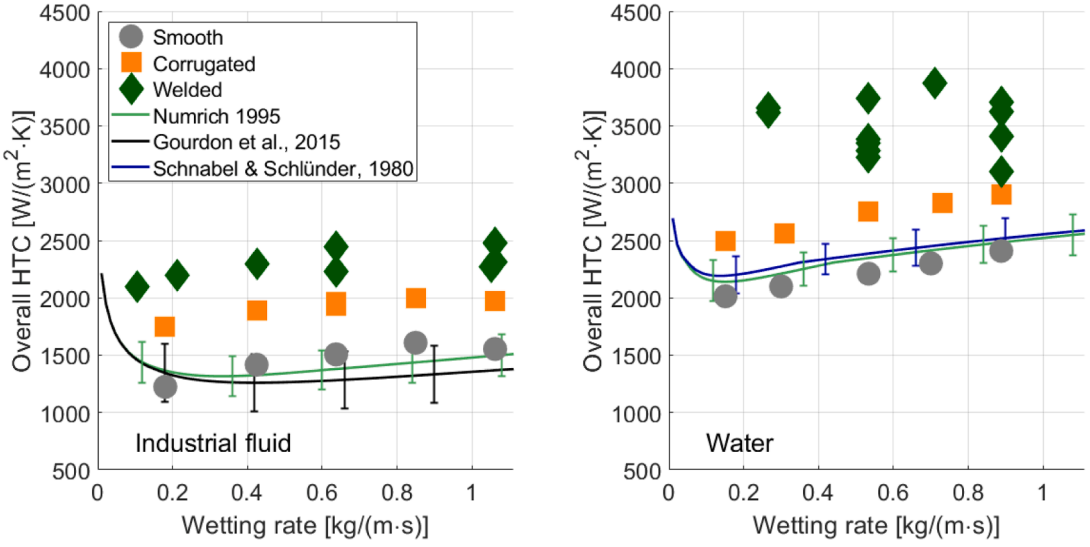

Fig. 6. Overall heat transfer coefficient (U) for the three heat transfer surfaces investigated for various wetting rates and at $\Delta T_{out} = 10$ K. Left) *Industrial fluid*, Right) *Water*.

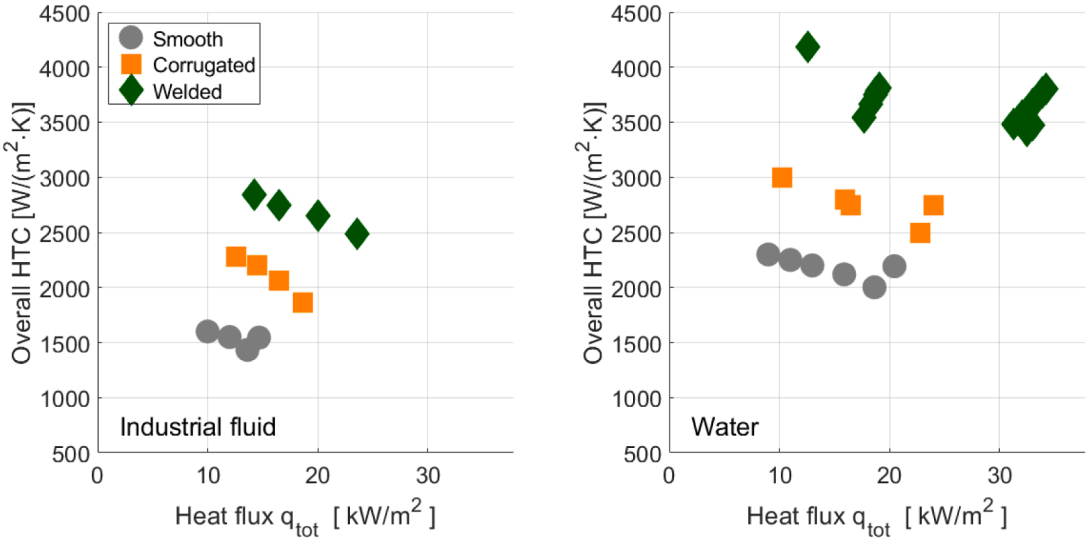

Fig. 7. Overall heat transfer coefficient (U) for the three heat transfer surfaces investigated for various heat fluxes, controlled by changing ΔT_{out}, more specifically T_{steam}. Left) *Industrial fluid*. Right) *Water*. The volumetric flow rate is 300 l/h for all measurements, which corresponds to a wetting rate of 0.63 and 0.53 kg/(m•s) for the fluids, respectively.

the *Welded* surface approximately 16% on the inside only. Also, especially in the latter case, it is questionable how much of the improvement is due to a probable fin efficiency in the surface modifications [2]. The observed heat transfer improvement is definitely much larger than that due to the sole effect of the increased surface area.

To understand the variation in the results, more operational conditions need to be added to the figures. If the area increase is neglected, the thermal driving force at the outlet ($\Delta T_{out} = T^*_{steam} - T_{out}$) can be visualized as straight lines in a heat flux graph (see Figs. 8 and 9). Since the pressure drop causes the thermal driving force to vary along the length of the tube, there is an uncertainty related to the averaged ΔT. Vertical error bars, with the maximum value equal to the overall heat transfer coefficient calculated from the inlet temperature difference ($\Delta T_{in} = T^*_{steam} - T^*_{in}$), can highlight this uncertainty. The overall heat transfer coefficient will of course never extend to the maximum value of the error bar, but it gives a representative understanding of how important the pressure drop is. The larger the error bar, the higher the impact of the pressure drop.

Eq. (5) can be used to estimate the magnitude of the evaporative heat transfer coefficient. By evaluating the heat transfer resistances for the wall and the condensing steam at 80 °C Eqs. (6) and ((7)), the overall HTC can be calculated for various values of the evaporative heat transfer coefficient (see Section 2.1). In addition, an infinite evaporative heat transfer coefficient represents a theoretical maximum value for the overall HTC, assuming that the correlations used to estimate the heat transfer resistance for the wall and the condensing steam are correct.

Fig. 8 shows all of the above visual representations added to the results presented in Fig. 7 for *Water*. Now it becomes clear that the previously seen heat flux dependence is strongly connected to the heat transfer resistance caused by the wall and the condensing steam. The

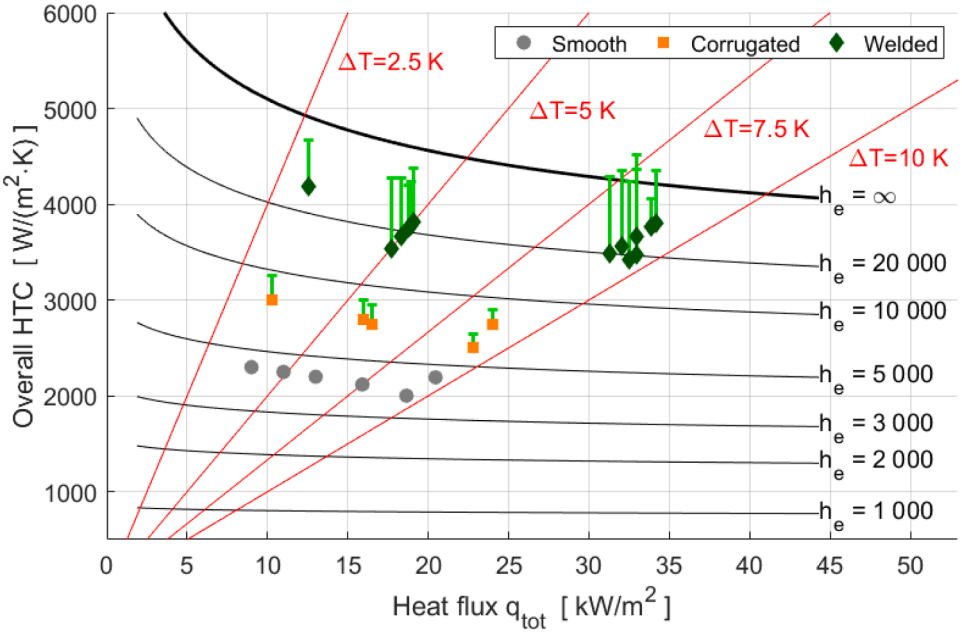

Fig. 8. Overall heat transfer coefficient (U) for *Water* as seen in Fig. 7. The thermal driving force, ΔT_{out}, and multiple evaporative heat transfer coefficients, calculated with Eq. (5), at a steam temperature of 80 °C, are added to the figure.

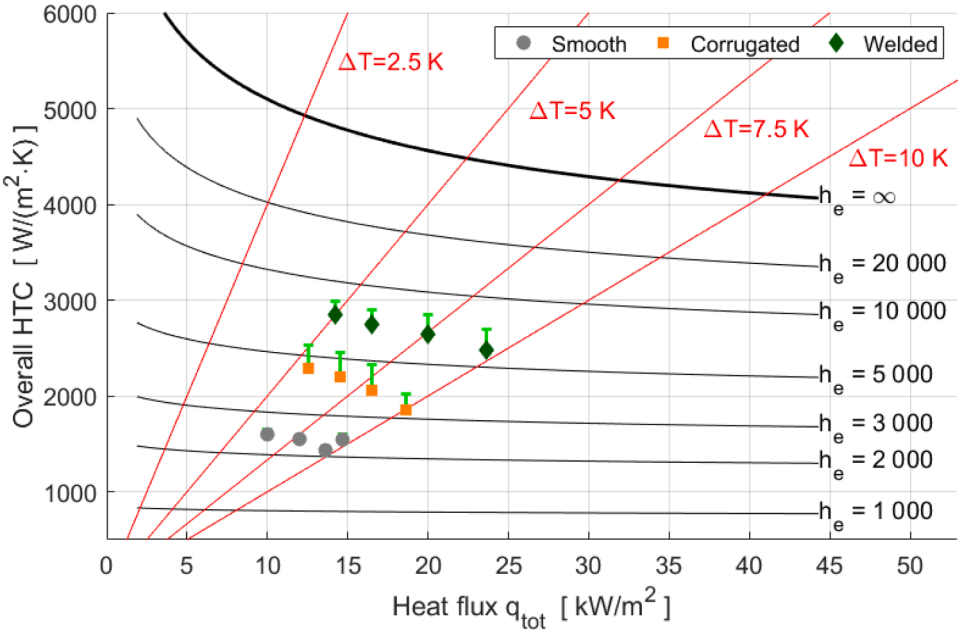

Fig. 9. Overall heat transfer coefficient (U) for the *Industrial fluid* as seen in Fig. 7. The thermal driving force, ΔT_{out}, and multiple evaporative heat transfer coefficients, calculated with Eq. (5), at a steam temperature of 80 °C, are added to the figure.

measurements, depending upon the modified surface used, follow either the 5 000 or the 20 000 $W/(m^2K)$ curve for the evaporative heat transfer coefficient. The values for the *Welded* surface are extremely high. As can be seen in the figure, multiple repetitions with the same outcome have been performed. Even the error bars slightly extend above the theoretical limit. It should be mentioned that the pilot evaporator was never designed to measure such high heat fluxes and there are thus reservations related to the obtained value. In addition, slight changes to the estimation of the heat transfer resistance from the wall and the condensing steam have an enormous impact on the evaporative heat transfer coefficient. Therefore, one should regard the heat transfer for *Water* on the *Welded* surface as high but interpret its exact value with caution.

Fig. 9 shows the same results but for the *Industrial fluid*. Here the heat flux dependence is stronger than for *Water* and it cannot solely be explained by the added resistance from the condensing steam and the wall. Gourdon, Innings, Jongsma and Vamling [25] found a positive heat flux dependence on smooth surfaces for dairy products, which the authors linked to the formation of bubbles, opposite to what is seen here on the modified surfaces. Also, their evaporative heat transfer coefficient varied between 2 200 and 3 200 $W/(m^2K)$ for loads between 3 and 14 kW/m^2, a span smaller than the one seen here. Further studies are thus needed to determine the precise cause to the heat flux dependence for the *Industrial fluid*.

At this stage, it is not meaningful with further data reduction into evaporative heat transfer coefficients and Nusselt numbers due to the fact that the exact influence of the pressure drop is unknown and much larger on the modified surfaces due to the increased rate of heat transfer. To investigate the pressure drop and its influence on the saturation temperature and the thermal driving force, the experimental setup needs to be adapted.

However, our results still indicate that the previously identified enhancement mechanism of increased bulk mixing due to the appearance of time-dependent recirculation zones behind the surface modifications could be plausible even for evaporation and not just heating.

In summary, our measurements demonstrate great potential for heat transfer improvement for falling film units with industrially relevant fluids by modifying heat transfer surfaces. It is also clear that, before any industrial implementation, further studies with a broader span of operating conditions, such as wetting rate, temperature, and various dry solid contents, are required to determine how a whole evaporation plant would be affected by the use of modified heat transfer surfaces. In addition, the possible effects of film breakage and dry spot formation necessitate further investigation as well. We, however, believe that the relevance of the pressure drop is a most interesting question here. The impact of the pressure drop on the saturation temperature, and hence the thermal driving force, will significantly vary at different operating temperatures due to the change to the specific volume of the vapor. Different tube lengths also need to be investigated as the vapour velocity will impact the pressure drop.

4. Conclusions

In this work we experimentally demonstrated, explained and quantified the potential for improvement of the rate of heat transfer when modified surfaces are used instead of smooth ones for vertical falling film evaporation. Our pilot-scale unit experiments show that the rate of heat transfer can indeed be significantly increased by the introduction of modified heat transfer surfaces.

The magnitude of the improvement depends on the design of modified surfaces and shows a slight wetting rate dependence. We have shown that the enhancement is also dependent on how the implementation is made and how the increase is interpreted, but, at the same heat flux, the improvement compared to a smooth surface is around 50% for the smoother *Corrugated* surface and up to 100% for the shaper *Welded* one. The pressure drop is higher on the modified surfaces, resulting in a lower thermal driving force. However, the analysis in this study has treated the pressure drop's effect conservatively, implying the highest possible theoretical increase of the thermal driving force, at least for this specific tube length. It is therefore possible that the improvement trends of utilizing the modified surfaces are even more pronounced, depending on the actual influence of the pressure drop on the thermal driving force.

CRediT authorship contribution statement

Anders Åkesjö: Conceptualization, Formal analysis, Investigation. **Mathias Gourdon:** Conceptualization, Investigation, Methodology.

Alfred Jongsma: Conceptualization, Investigation, Methodology. **Srdjan Sasic:** Conceptualization, Investigation, Project administration, Supervision.

Declaration of Competing Interest

The authors declare that they have no known competing financial interests or personal relationships that could have appeared to influence the work reported in this paper.

Acknowledgments

This work was co-funded by the Swedish Energy Agency, Valmet AB and Tetra Pak Processing systems.

References

[1] G. Schnabel, Heat transfer to falling films at vertical surfaces, in: VDI-GVC (ed.). VDI Heat Atlas, 2nd ed., Springer, Berlin, 2010.
[2] R.L. Webb, N.H. Kim, Principles of Enhanced Heat Transfer, 2nd ed, Taylor & Francis, Great Britain, 2005.
[3] L.A. Miriam, Experiments On Falling Film Evaporation of a Water-Ethylene Glycol Mixture On a Surface With Longitudinal Grooves, Institut für Energietechnik, Technischen Universität Berlin, Berlin, 2007 in:.
[4] T. Gambaryan-Roisman, P. Stephan, Analysis of falling film evaporation on grooved surfaces, J. Enhanc. Heat Transf. 10 (2003) 445–457.
[5] T. Gambaryan-Roisman, H. Yu, K. Löffler, P. Stephan, Long-wave and integral boundary layer analysis of falling film flow on walls with three-dimensional periodic structures, Heat Transf. Eng. 32 (2011) 705–713.
[6] N. Pecherkin, A. Pavlenko, O. Volodin, Heat transfer and crisis phenomena at the film flows of freon mixture over vertical structured surfaces, Heat Transf. Eng. (2015) 1–12.
[7] H. Li, F. Yi, X. Li, A.N. Pavlenko, X. Gao, Numerical simulation for falling film flow characteristics of refrigerant on the smooth and structured surfaces, J. Eng. Thermophys. 27 (2018) 1–19.
[8] D. Slade, S. Veremieiev, Y.C. Lee, P.H. Gaskell, Gravity-driven thin film flow: the influence of topography and surface tension gradient on rivulet formation, Chem. Eng. Process. 68 (2013) 7–12.
[9] H. Yu, K. Löffler, T. Gambaryan-Roisman, P. Stephan, Heat transfer in thin liquid films flowing down heated inclined grooved plates, Comput. Therm. Sci. 2 (2010) 455–468.
[10] M. Najim, M.B. Feddaoui, A. Nait Alla, A. Charef, Computational study of liquid film evaporation along a wavy wall of a vertical channel, Math. Probl. Eng. 2018 (2018) 1–11.
[11] H. Raach, J. Mitrovic, Seawater falling film evaporation on vertical plates with turbulence wires, Desalination 183 (2005) 307–316.
[12] W.M. Salvagnini, M.E.S. Taqueda, A falling-film evaporator with film promoters, Ind. Eng. Chem. Res. (2004) 43.
[13] L. Broniarz-Press, Enhancement of mass transfer coefficients in spiral films, Int. J. Heat Mass Transf. 40 (1997) 4197–4208.
[14] Z.Q. Shen, Effect of systematic grooved surface on the rate of heat and mass transfer in a falling liquid film, in: Proceedings of the 8th International Heat Transfer Conference, 1986, pp. 1957–1962. Vol. 4, San Francisco, USA.
[15] G.S. Zheng, W.M. Worek, Method of heat and mass transfer enhancement in film evaporation, Int. J. Heat Mass Transf. 39 (1996) 97–108.
[16] A. Ramadane, P.L. Goff, B. Liu, The enhancement of heat transfer in falling film evaporators by a non-uniform flow rate, Energy Effic. Process Technol. (1993).
[17] H.L. Goff, A. Soetrisnanto, B. Schwarzer, P.L. Goff, A new falling film evaporator with spiral fins, Chem. Eng. J. 50 (1992) 169–171.
[18] P. Bandelier, Improvement of multifunctional heat exchangers applied in industrial processes, Appl. Therm. Eng. 17 (1997) 777–788.
[19] M. Kohrt, Experimentelle untersuchung von stofftransport und fluiddynamik bei rieselfilmströmungen auf mikrostrukturierten oberflächen, Vol.. Doktor Der Ingenieurwissenschaften, ProzesswissenschaftenTechnischen Universität Berlin, Berlin, 2012.
[20] L. Zhao, R.L. Cerro, Experimental characterization of viscous film flows over complex surfaces, Int. J. Multiph. Flow 18 (1992) 496–516.
[21] J.J. Schröder, P. Fast, W. Sander-Beuermann, Hydrodynamics and heat transfer on vertically finned surfaces in falling film evaporators, Desalination 31 (1979) 19–34.
[22] K. Helbig, R. Nasarek, T. Gambaryan-Roisman, P. Stephan, Effect of longitudinal minigrooves on flow stability and wave characteristics of falling liquid films, Trans. ASME: J. Heat Transf. 131 (2009).
[23] A. Åkesjö, M. Gourdon, L. Vamling, F. Innings, S. Sasic, Modified surfaces to enhance vertical falling film heat transfer – an experimental and numerical study, Int. J. Heat Mass Transf. 131 (2019) 237–251.
[24] G. Schnabel, E.U. Schlünder, Wärmeübergang von senkrechten wänden an nichtsiedende und siedende rieselfilme. "heat transfer from vertical walls to falling liquid films with or without evaporation, Verfahrenstechnik 14 (1980) 79–83.
[25] M. Gourdon, F. Innings, A. Jongsma, L. Vamling, Qualitative investigation of the flow behaviour during falling film evaporation of a dairy product, Exp. Therm Fluid Sci. 60 (2015) 9–19.
[26] S. Bouman, R. Waalewijn, P.D. Jong, H.J.L.J.V.D. Linden, Design of falling-film evaporators in the dairy industry, J. Soc. Dairy Technol. 46 (3) (1993) 100–106.
[27] E. Mura, M. Gourdon, Pressure drop in dairy evaporators: experimental study and friction factor modelling, J. Food Eng. 195 (2017) 128–136.
[28] I. Zadrazil, C.N. Markides, An experimental characterization of liquid films in downwards co-current gas–liquid annular flow by particle image and tracking velocimetry, Int. J. Multiph. Flow 67 (2014) 42–53.
[29] M. Gourdon, E. Mura, Performance evaluation of falling film evaporators in the dairy industry, Food Bioprod. Process. 101 (2017) 22–31.
[30] M. Johansson, I. Leifer, L. Vamling, L. Olausson, Falling film hydrodynamics of black liquor under evaporative conditions, Int. J. Heat Mass Transf. 52 (2009) 2769–2778.
[31] M. Johansson, L. Olausson, L. Vamling, A new test facility for black liquor evaporation, Heat Transf. Compon. Syst. Sustain. Energy Technol. (2005).
[32] M. Gourdon, E. Karlsson, F. Innings, A. Jongsma, L. Vamling, Heat transfer for falling film evaporation of industrially relevant fluids up to very high prandtl numbers, Heat and Mass Transf. 52 (2015) 379–391.
[33] E. Karlsson, M. Gourdon, L. Vamling, The effect of bulk crystals on sodium salt scaling in black liquor evaporators, Nord. Pulp Pap. Res. J. 32 (2017) 299–308.
[34] Sacome, Corrugated tube heat exchangers, in: Corrugation Technol. (2023) 2023. VolSacome, Sacome.com.
[35] NIST, NIST Chemistry WebBook. NIST Chemistry WebBook, Vol. 2017, U.S Department of Commerce, United States of America, 2017.
[36] T.N. Adams, W.J. Frederick, T.M. Grace, M. Hupa, K. Lisa, A.K. Jones, H. Tran, Kraft Recovery Boilers, American Forest & Paper Association, New York, 1997, p. 381.
[37] P. Cyklis, Industrial scale engineering estimation of the heat transfer in falling film juice evaporators, Appl. Therm. Eng. 123 (2017) 1365–1373.
[38] VDI Heat Atlas, 2 ed, Springer, Berlin, Heidelberg, 2010.
[39] M.J. Assael, K. Gialou, Measurement of the thermal conductivity of stainless steel AISI 304L up to 550K, Int. J. Thermophys. 24 (4) (2003) 1145–1153.
[40] R. Numrich, J. Müller, Filmwise condensation of pure vapors, in: In. VDI-GVC (ED., SpringerVDI Heat Atlas, Berlin, 2010.
[41] M. Johansson, L. Vamling, L. Olausson, Falling film evaporation of black liquor - comparison with general heat transfer correlations, v 21 (2006) 496–506.
[42] R. Numrich, Heat transfer in turbulent falling films, Chem. Eng. Technol. 18 (1995) 171–177.
[43] I. Zadrazil, O.K. Matar, C.N. Markides, An experimental characterization of downwards gas–liquid annular flow by laser-induced fluorescence: flow regimes and film statistics, Int. J. Multiph. Flow 60 (2014) 87–102.